I.O.S.

COMPARISONS OF THE METEOROLOGICAL OFFICE AND NORSWAM WAVE MODELS WITH MEASURED WAVE DATA COLLECTED DURING MARCH 1980

by

J A EWING J J EPHRAUMS
B W GOLDING AND B A WORTHINGTON

REPORT NO 127

1981

NATURAL ENVIRONMENT RESEARCH COUNCIL

INSTITUTE OF OCEANOGRAPHIC SCIENCES

INSTITUTE OF OCEANOGRAPHIC SCIENCES

Wormley, Godalming,
Surrey, GU8 5UB.
(0428 - 79 - 4141)

(Director: Dr. A.S. Laughton)

Bidston Observatory,
Birkenhead,
Merseyside, L43 7RA.
(051 - 653 - 8633)

(Assistant Director: Dr. D.E. Cartwright)

Crossway,
Taunton,
Somerset, TA1 2DW.
(0823 - 86211)

(Assistant Director: M.J. Tucker)

COMPARISONS OF THE METEOROLOGICAL OFFICE AND NORSWAM WAVE MODELS WITH MEASURED WAVE DATA COLLECTED DURING MARCH 1980

J.A. Ewing*, J.J. Ephraums+, B.W. Golding+ and B.A. Worthington‡

Report No. 127

1981

Prepared for the Wave Energy Steering Committee
and supported by the Department of Energy, July 1981

* Institute of Oceanographic Sciences, Wormley, Surrey
+ Meteorological Office, Bracknell, Berkshire
‡ Hydraulics Research Station, Wallingford, Oxfordshire

SUMMARY

The purpose of this work was to assess the ability of two numerical wave models to estimate wave power characteristics at deep water positions along the U.K. continental shelf.

The Meteorological Office and NORSWAM wave models were used with the same input wind field continuously for one month. Model results were compared with wave height and wave power estimates derived from wave measurements at five stations.

1. INTRODUCTION

During the last few years two new numerical wave models have been developed. The North Sea Wave Model (NORSWAM) group have used a parametrical wave model to hindcast extreme value wave heights for severe storms over a 10-year period (Ewing, Weare and Worthington, 1979). At the same time, B.W. Golding at the Meteorological Office had developed a source function model for use in routine wave prediction and he has demonstrated the use of this model in estimating average monthly wave power levels (Golding, 1980 a).

The present study compares results from these two wave models using the same input wind field for March 1980, determined by the Meteorological Office, Bracknell. The model results have been compared with wave statistics derived from spectral estimates at five, deep water, stations, around the British Isles, namely Brent B, Kinnaird's Head, South Uist, O.W.S. Lima and DB1.

Previous studies of wave power around the British Isles have mainly been based on wave measurements at a few stations and have therefore concentrated on temporal variations in wave power levels. A wave model which can give reliable estimates of wave power would be of considerable use in estimating both the spatial and temporal variability of power along the U.K. continental shelf.

2. DESCRIPTION OF METEOROLOGICAL OFFICE MODEL

The operational wave prediction model used by the U.K. Meteorological Office has a grid point representation of the wave field. This is usually defined on a Polar Stereographic projection of the earth's surface and it can be initialised with any gridlength and any shape or size of ocean basin subject to computer core storage constraints. It has a general nesting capability permitting any model to obtain inflow boundary conditions from any other. Operationally, two models are run. One covers much of the Northern Hemisphere with a gridlength at 60^{O}N of 300 kms. This provides boundary conditions for a 50 km

gridlength model of the Northwest European Continental Shelf. Fig. 1 shows the region covered by that model together with adjacent gridpoints of the course mesh model used for boundary conditions.

The wave field at each point is described by a discrete spectrum. The spectral resolution is variable but at present comprises 12 direction components (30^{o} resolution) and 11 frequencies (0.05, 0.06, 0.072, 0.086, 0.104, 0.124, 0.148, 0.178, 0.214, 0.256, 0.308 Hz). Shallow water effects are included only in the continental shelf model. They are calculated on a 2 metre depth resolution and model the influence of variable group velocity, refraction, and bottom friction. They have a significant effect on the results in the North Sea and English Channel.

The model solves the energy balance equation (where E is the directional wave spectrum and S the source function)

$$\frac{dE}{dt} = S(E)$$

starting from initial conditions which may be zero or prescribed by the results of the last integration; and subject to radiative boundary conditions with zero inflow at coasts and prescribed inflow at open sea boundaries. The balance equation is actually solved in the following form

$$\underbrace{\frac{\partial}{\partial t}(E_{ij})}_{(i)} = \underbrace{-\nabla.(\underline{c}_g E_{ij})}_{(ii)} \underbrace{-\frac{\partial}{\partial \theta}\{(\underline{c}_g.\nabla\theta E_{ij}\}}_{(iii)} + \underbrace{\alpha + \beta E_{ij} - \Delta(E)}_{(iv)} + \underbrace{\Gamma(E)}_{(v)} - \underbrace{\Phi(E)}$$

Multiplicative splitting is used so that integration of each numbered section uses the results of the previous section. An attempt has been made above to indicate those parts which operate on the uncoupled spectral components (E_{ij}) and those which operate on the whole spectrum (E). The detailed form of each term is given below. A variable timestep is used in the model. The basic timestep is equal to the time interval between successive updates of the wind field. Divisors and multiples of this timestep are used in section (i), (ii) such that the

stability criterion for each frequency component in the propagation scheme is always satisfied. In practice this means that the ratio of gridlength to timestep varies between about 0.4 and 0.8 of the deep water group velocity.

(i) Propagation $$\frac{\partial}{\partial t}(E_{ij}) = -\nabla.(\underline{c}_g E_{ij})$$

This term is integrated using a modified Lax-Wendroff integration scheme. For one dimensional propagation at constant speed c it takes the form

$$E_{j+\frac{1}{2}}^{n+\frac{1}{2}} = 0.5(E_j^n + E_{j+1}^n) - \frac{\mu}{2}(E_{j+1}^n - E_j^n)$$

$$E_j^{n+1} = E_j^n - \mu\left\{(1+a)(E_{j+\frac{1}{2}}^{n+\frac{1}{2}} - E_{j-\frac{1}{2}}^{n+\frac{1}{2}}) - \frac{a}{3}(E_{j+\frac{3}{2}}^{n+\frac{1}{2}} - E_{j-\frac{3}{2}}^{n+\frac{1}{2}})\right\}$$

where $\mu = c\Delta t/\Delta x$, $a = \frac{3}{4}(1-\mu^2)$, j signifies spatial position and n the time level. For details of its derivation see Gadd (1978) and for its application to the wave model see Golding (1977).

(ii) Refraction $$\frac{\partial}{\partial t}(E_{ij}) = -\frac{\partial}{\partial \theta}\left\{(\underline{c}_g.\nabla\theta)E_{ij}\right\}$$

The refraction scheme is based on Snell's law for optical refraction and details of the derivation are given in Golding (1977, 1978 a). The resultant form for $\underline{c}_g.\nabla\theta$ may be written

$$\underline{c}_g.\nabla\theta = -\frac{|\underline{c}_g|}{k}\left[\frac{\partial H}{\partial x}\sin\theta - \frac{\partial H}{\partial y}\cos\theta\right]\left[\frac{-k^2\,\mathrm{sech}^2 kH}{\tanh kH + kH\,\mathrm{sech}^2 kH}\right]$$

where H is water depth and k is wave number. The numerical scheme uses centred differences in θ, the direction of the wave component being operated on.

(iii) Growth and Decay $$\frac{\partial}{\partial t}(E_{ij}) = \alpha + \beta E_{ij} - \Delta(E)$$

The α term initiates wave growth but is unimportant thereafter. A simple form is used which removes the effects of variable spectral resolution:

$$\alpha = \begin{cases} \alpha_1 U^2 \cdot \frac{2}{\pi} \cos^2(\theta-\psi) & \text{for highest frequency if } |\theta-\psi| \leq 90^\circ \\ 0 & \text{otherwise} \end{cases}$$

where U, ψ is the wind speed and direction.

The β term gives exponential growth. It has a cut-off for waves travelling faster than the wind.

$$\beta = \begin{cases} \beta_1 2\pi f \left[U\cos(\theta-\psi)/V_f - 1\right] & \text{if } \frac{U\cos(\theta-\psi)}{V_f} > 1 \\ 0 & \text{otherwise} \end{cases}$$

where $V_f = g/2\pi f$ is the deep water phase speed of the waves.

Dissipation is based on Hasselmann's white-capping model (1974),

$$\Delta(E) = \Delta_1 f^2 \bar{E}^{0.25} E_{ij}$$

where $\bar{E}$ is the total spectral energy.

(iv) Non-linear interactions $\frac{\partial E_{ij}}{\partial t} = \Gamma(E)$

The wind sea part of the spectrum is first separated from the rest. It is then assumed that the non-linear interactions will act to transform this into a JONSWAP spectrum directionally centred on the wind direction, with peak frequency and peak enhancement uniquely related to the energy in the wind sea regime. (Hasselmann et al. 1973). The spectrum is transformed to this shape with the total energy conserved. The transformation is immediate and couples all components with frequency greater than 0.8 of the peak, and direction within 90° of the wind. For a detailed description see Golding (1980 b).

(v) Bottom friction $$\frac{\partial E_{ij}}{\partial t} = -\Phi(E)$$

This is based on Collins' formulation for quadratic bottom friction (1972),

$$\Phi(E) = \frac{\Phi_1 g k |c_g|}{2\pi f^2 \cosh^2 kH} \left\{ \iint \frac{g^2 k^2 E_{ij}\, d\theta\, df}{f^2 \cosh^2 kH} \right\}^{1/2} \cdot E_{ij}$$

Wind input is obtained from the operational numerical atmospheric prediction system of the U.K. Met. Office. For the diagnosis of the present sea state a number of sources of information are used. The most recent forecast for the past twelve hours forms the basis. This is corrected at the end of the period by winds derived from the operational pressure analysis. Finally, it is corrected every three hours by insertion of wind observations using a two parameter orthogonal polynomial analysis (see Golding 1978 b). Finally, the corrections are applied in linearly decreasing amounts away from the observation times. The forecast and analysis values of wind are obtained from the 900 mb fields (U_{900}, ψ_{900}) by applying formulae derived from Findlater et al.(1966),

$$U = a\, U_{900}^2 + b\, U_{900} + c$$

$$\psi = \psi_{900} + d$$

where a, b, c, d are stability dependent constants. These equations provide 19.5 metre winds (U, ψ). No corrections for height are made to the observations.

3. DESCRIPTION OF THE NORSWAM MODEL

Results from the JONSWAP study (Hasselmann et al. 1973) have shown that the non-linear wave-wave interactions, in conjunction with the energy input from the atmosphere, have a shape stabilising effect on the wind-sea part of the spectrum, thus giving rise to the mean JONSWAP spectral shape. In addition, the dynamic balance between the non-linear interactions and the atmospheric

input means that the direction of the wind-sea spectrum tends to follow the wind direction (Hasselmann et al, 1976).

Under these conditions, the directionally integrated energy balance equation (for deep water)

$$\frac{\partial E}{\partial t} + \underline{v} \cdot \nabla E = S$$

where

$E = E(f)$ = energy density, f being frequency
v = directionally integrated group velocity
S = Source function

can be projected into the JONSWAP parameter space as

$$\frac{\partial a_i}{\partial t} + D_{ij} \frac{\partial a_j}{\partial x} = T_i \quad (i = 1, \ldots, 5)$$

where

a_i are the JONSWAP five free parameters ($f_m, \alpha, \gamma, \sigma_a, \sigma_b$)
D_{ij} is a generalised propagation velocity
T_i is the projection of the source term S.

(for further details, see Günther et al., 1979).

In this form, the normally complicated nonlinear interactions take a simple theoretical form. The atmospheric input term is based on a Miles (1957) formulation, adjusted to agree with observations. In the NORSWAM model, only three parameters are free; σ_a and σ_b are held fixed at their mean JONSWAP values. It was found that the extra accuracy obtained from using the full five parameters was negligible. The parametrical equations are solved using a Lax-Wendroff finite difference scheme.

The above approach breaks down in the swell region of the spectrum where the non-linear interactions are negligible; without their shape stabilising influence the parametrical form of E no longer applies and individual wave components become almost completely decoupled. Swell is therefore treated using a characteristic ray method, with swell energy being advected along predetermined straight wave rays.

The overall model is thus hybrid, with energy being transferred between swell and wind-sea fields as either swell becomes absorbed by a growing wind-sea in a rising wind, or energy from the wind-sea is lost to swell when the wind falls.

4. CONDUCT OF THE NUMERICAL EXPERIMENT

The object of the experiment was to compare the two wave models in a real time forecasting environment. In order to achieve this, the NORSWAM model was modified so that it would run on the same geographical grid and use the same wind input and boundary conditions as the Met. Office model. The finite difference grid of the NORSWAM model was given the same resolution and coastline definition as that shown in Fig 1. For the characteristic rays, a spacing of one gridlength in the coordinate directions was maintained except for remote corners of the area where a two gridlength spacing was used. The swell bins of the NORSWAM model were defined to have the same spectral resolution as those used in the Met. Office model up to a frequency of 0.178 Hz. The input of boundary conditions was achieved by assigning incoming spectral energies to the swell bins. The model itself then computed the appropriate transfer to the wind sea. Both at this stage and in the output, units of spectral energy were converted between m^2 in NORSWAM and $m^2\ (\mathrm{Hz\ rad})^{-1}$ in the Met. Office model.

Although the intention was to run the NORSWAM model in real time alongside the Met. Office model, operational difficulties and a desire to perform the comparison on a winter month caused this to be abandoned. Instead, the wind fields and boundary conditions for March 1980 were copied to magnetic tape in real time and the model run later. A small number of losses of data occurred during this process. They are listed, together with the action taken, in Table 1. During the month, results of the Met. Office model were stored at six-hourly intervals in a compact form used for routine archiving. In this form, each spectral energy component is stored in integer form, rounded to the nearest $m^2\ (\mathrm{Hz\ rad})^{-1}$. This is unimportant near the spectral

peak but introduces a low bias in high frequency components which affects the computation of high order moments of the spectrum. Results from the NORSWAM model were stored in full at 24hr intervals. At 6 hr intervals they were first converted to the same form as output from the Met. Office model. This was done by evaluating the JONSWAP spectrum describing the parametrical wind-sea at the frequencies and directions of the discrete spectrum and adding energy from the swell bins to the appropriate components. These results were then stored in the same compact form as the Met. Office model output. Standard programs were then available both for output of the results in chart form, and for extracting the time series at specific locations from which the analysis in section 7 was made.

5. GENERAL WEATHER SITUATION FOR MARCH 1980

The weather of March 1980 began with an anticyclone just west of the British Isles and strong northerly winds over the North Sea, particularly on the 2nd at Brent B. On the 3rd and 4th this high pressure area moved south-eastwards and a new anticyclone established itself over the Azores where it remained until the 14th. During this period a succession of vigorous North Atlantic depressions and fronts crossed the British Isles bringing extremely unsettled weather and frequent strong gales (see OWS Lima, in Fig. 2 for example).

On the 6th and 7th a particularly deep depression moved south-eastwards across the British Isles giving rise to strong north-westerly gales at OWS Lima and DB1 (see Fig.2). For the next eight days a low pressure area was positioned between Greenland and Iceland whilst further small cyclones, and fronts, crossed northern parts of the British Isles.

The 11th was an especially active day, when the strongest winds of the month were recorded at Brent B and OWS Lima, and both Kinnairds Head and South Uist experienced near-maximum winds for this month.

Between the 14th and 16th there was a significant change

in the general weather pattern as the Azores anticyclone moved north-west to establish a general area of high pressure over Greenland for most of the month remaining. Also by the 16th a ridge of high pressure had extended from Scandinavia to cover most of the British Isles, and this change brought a quiet spell to all but the more western areas such as South Uist and OWS Lima.

On the 17th, however, a weak cyclone formed over the British Isles which drifted to the south during the next two days leaving a strong easterly flow over the North Sea and western sea areas. On the 21st another cyclone began to develop over the British Isles and the following day saw strong south-easterly winds over much of the North Sea with Kinnairds Head recording its highest values for this month, whilst the other stations remained largely unaffected. By the 23rd the depression had become a large feature just west of Ireland and it remained in this position until the 25th, accompanied by moderate but settled wind conditions.

On the 26th the area of low pressure moved northwards to become a weaker feature and during the next two days an area of slack pressure prevailed north-west of the British Isles which produced settled calm winds in this area (see Fig. 2, OWS Lima, South Uist). However, further south the situation was mobile, with small mid-Atlantic depressions crossing southern parts of the British Isles until a dominant cyclone reached the British Isles by the 31st bringing stronger winds once more to most parts. In particular, the strongest winds of the month were recorded at South Uist on the last day.

Table 2 shows the number of days during which a specified wind speed was exceeded at the five stations for which wave measurements were available.

6. MEASURED WAVE DATA

Measured wave data at five stations were used to compare with the model predictions. Table 3 gives details of the positions of the stations and of the wave recorders used to obtain the data.

For Brent B the significant wave height, h_s, and mean zero-crossing period T_z were obtained from a processor which derived

these quantities directly from the analogue signal.

In the case of the other four stations, wave spectral information were available and the estimation of significant wave height, zero-crossing period and wave power, P, were derived from calculations of the moments of the spectrum E(f), namely

$$h_s = 4\sqrt{m_0} \qquad (m)$$

$$T_z = \sqrt{(m_0/m_2)} \qquad (sec.)$$

$$P = 7.85\, m_{-1} \qquad (kW/m)$$

where the moments of the spectrum were computed from

$$m_n = \sum_{f=.05\,Hz}^{f_1} f^n E(f) \Delta f$$, with wave frequency, f, in Hz.

The upper limit of summation depends on the reliability of high frequency information from a given wave recorder and this was chosen as

$$f_1 = \begin{cases} 0.25 \text{ Hz} & \text{for SBWR} \\ 0.42 \text{ Hz} & \text{for DB 1} \\ 0.68 \text{ Hz} & \text{for Waverider} \end{cases}$$

In the calculation of the wave spectrum, standard analysis methods using the Fast Fourier Transform were employed. In all cases $\Delta f = 0.01 Hz$; degrees of freedom of spectral estimates were 20 for the waverider measurements and 24 for DB1.

For the shipborne wave recorder (SBWR) the heave and pressure signals were recorded separately. The pressure signal was then transformed to a sensor at a depth of 2.5 times the actual depth (1.84 m) of the transducer. Finally the heave and modified pressure were combined to give an estimate of wave height. (E.G. Pitt; personal communication).

7. MODEL WAVE DATA

The model wave data were output on magnetic tape in the form of variance elements associated with a given frequency and

and direction. After integration over direction, the spectral energy densities, E(f), from both models were available at eleven frequencies centred at 0.05, 0.06, 0.072, 0.086, 0.104, 0.124, 0.148, 0.178, 0.214, 0.256 and 0.308Hz respectively. The bandwidths associated with these frequencies vary from Δf = 0.01Hz at the lowest frequency to Δf = 0.052 Hz at the highest frequency.

Moments of the spectrum were computed as in Section 6 but with upper limits of f_1 = 0.214 Hz (Met. Office) and f_1 = 0.308 Hz (NORSWAM).

Model grid points do not coincide with the measurement stations. It was therefore decided to average the results from the two nearest grid points to compare with each measurement station. However, in the case of OWS Lima the nearest grid point was used since this was less than 12 km away from the measurement station.

8. RESULTS OF THE COMPARISONS

Comparison of the wave model results with wave measurements are shown in the form of time series (Figs. 3-7) and in the form of graphs (Figs 8-12) showing the correlations of model with measured values. In the case of wave power a logarithmic scale, starting at 10 kW/m, was used to eliminate uninteresting low levels of wave power.

Table 4 gives values of the least squares fit of parameters relating model and measured values of wave height and wave power; the least squares fit is constrained to pass through the origin. Table 5 shows the results for a general least squares fit thus giving both gradient and intercept of the fitted straight line.

There was very poor correspondence between both models and measured estimates of wave period (see Figs. 8-12) and the variation of T_z throughout the month has therefore been omitted from the time series plots. (Parameters of a least squares fit

for wave period are also not included in Tables 4 and 5). To some extent this lack of agreement between estimates of wave period is due to the influence of the high frequency tail in the wave spectrum and depends on the truncation frequency f_t (see, for example, Rye (1977)).

(a) Brent B.

Both models agree quite well with measured significant wave heights throughout the month, as shown in Fig. 3 (Wave power estimates were not available at this station). For the period 1-13 March the Met. Office model gives results close to the measurements while NORSWAM tends to overpredict the values of significant wave height.

For the remainder of the month both models exhibit similar close agreement with the measurements. The high wave heights on 3 and 12 March are well predicted by both models.

The correlation diagram (Fig. 8) confirms the good agreement between model and measured significant wave height. Values of the standard error of residuals given in Tables 4 and 5 indicate a marginally better agreement with the measurements for the Met. Office model than NORSWAM for significant wave height.

(b) Kinnaird's Head.

The Met. Office model agrees well with measured significant wave height and power (Fig. 4) except for a short period on 2 and 3 March. The NORSWAM model tends to underestimate wave heights and power during the two periods 12-15 March and 25-28 March. Both models correctly predict the high wave heights and power on 22 March. The standard errors in Tables 4 and 5 are smaller for the Met. Office model than for NORSWAM.

(c) South Uist.

Both models overestimate wave height and power levels especially during the three periods 1-4, 11-14 and 28-30 March when the wave heights are greatest (Fig. 5). This discrepancy is probably due to the closeness of the nearest grid point to land where the coastal boundary is not adequately defined on a

50 km mesh. Although the Met. Office model includes both dissipation and refraction for shallow water, these influences do not appear to be important at South Uist (where the depth at the measurement station is 42 m) since the NORSWAM results agree closely with the Met. Office output for these two periods. This is confirmed by values of the parameters in Tables 4 and 5.

(d) O.W.S. Lima.

Unfortunately, the most interesting period for comparison (9-15 March) is missing from the measurements (see Fig. 6).

The high wave heights and power levels during the first eight days of March are well predicted by the NORSWAM model; the Met. Office model underpredicts the values during the period 7-9 March. For the remainder of the month (16-31 March) both models agree reasonably well with the measurements although the rapid decrease in measured wave power on 17-18 March is not adequately followed by either model.

Tables 4 and 5 and Fig. 11 indicate that the NORSWAM results are closer to a 1:1 linear relation than the Met. Office model which has an intercept of about 2 m for the two parameter fit.

(e) DB1.

Both models agree quite well with measured significant wave height and power throughout the month although the NORSWAM model overpredicts some values during the period 5-13 and 23-25 March (Fig. 7).

The high wave heights and power levels on 7 March (12½ m and 1000 kW/m respectively) from both models are in close agreement with the measurements.

Tables 4 and 5 confirm the better agreement from the Met. Office model compared with NORSWAM.

9. CONCLUSIONS

In general, both models agree quite well with the measured wave data with the exception of comparisons at South Uist. At South Uist the proximity of the coastline and the coarse mesh size of 50 km. appears to be the reason for the discrepancies of both

models compared with measurements. Both models also share the same boundary values derived from the coarse mesh model on a 300 km grid. Errors in the specification of swell in particular would propagate from the boundaries and contaminate both model results. The poor performance of both models at South Uist on some occasions may be due to this effect.

In many cases both models give very similar results showing that one of the main factors influencing wave prediction is an accurate specification of the wind field. At Brent B and Kinnaird's Head, the waves are generated by local winds with little extraneous swell present; in this situation there is generally good agreement with the measurements. At the open ocean stations, we would expect the wind fields to be better represented for oceanic conditions west of DB1 than at OWS Lima due to the greater number of selected ship reports near the former position. There is some indication that this is the case from estimates of the gradient of the line in the two-parameter regression (Table 5).

The highest wave heights and wave power values (in one case in excess of 12 m. and 1200 kW/m respectively) are well-predicted by both models.

The standard errors of model estimates vary from 0.6 m at Kinnaird's Head (in the North Sea) to about 1.4 m at DB1 (in the Western Approaches). Corresponding values of wave power are about 20 kW/m and 140 kW/m at these two stations.

10. ACKNOWLEDGEMENTS

This work was supported financially by the Department of Energy to provide information on wave modelling techniques relevant to the Wave Energy Programme.

Measured wave data used for comparative purposes have been kindly supplied by Shell U.K. Exploration & Production (at Brent B), the Institute of Oceanographic Sciences, Taunton (at Kinnaird's Head, South Uist and O.W.S. Lima) and the U.K. Offshore Operators Association (at DB1).

The authors thank their colleagues P.J. Challenor, P.E. Francis and E.G. Pitt for their helpful advice and assistance.

11. REFERENCES

COLLINS, J., (1972). Prediction of shallow water spectra. J. Geophys. Res. 77, 2693-2707.

EWING, J.A., T.J. WEARE and B.A. WORTHINGTON, (1979). A hindcast study of extreme wave conditions in the North Sea. J. Geophys. Res., 84, 5739-5747.

FINDLATER, J.; HARROWER, T.N.S., HOWKINS, G.A. and WRIGHT, H.L. (1966). Surface and 900mb wind relationships. Met. O. Sci. Pap. 23. HMSO, London.

GADD, A.J. (1978). A numerical advection scheme with small phase speed errors. Quart. J.R. Met. Soc., 104, 583-594.

GOLDING, B.W. (1977). A depth dependent wave model for operational forecasting, in "Turbulent fluxes through the sea surface, wave dynamics and prediction." Ed. A. Favre &. K. Hasselmann. Plenum Press, New York, 593-604.

GOLDING, B.W. (1978a). The inclusion of refraction and shoaling in the Meteorological Office Wave Forecast model. Met. O. 2B Tech. Note No. 53*.

GOLDING, B.W. (1978 b). A proposed surface wind analysis system for the fine mesh wave forecast. Met. O. 2B Tech. Note No. 54*.

GOLDING, B.W. (1980 a). Computer calculations of waves from wind fields. In "Power from Sea Waves". Proc. of a conference held in June 1979. Edited by B. Count, 115-134.

GOLDING, B.W. (1980 b). The Modelling of wave growth & decay in the Meteorological Office Operational wave model. Met. O. 2B Tech. Note No. 76*.

GUNTHER, H., W. ROSENTHAL, T.J. WEARE and B.A. WORTHINGTON, K. HASSELMANN and J.A. EWING. (1979). A hybrid parametrical wave prediction model. J. Geophys. Res., 84, 5727-5738.

HASSELMANN, K., T.P. BARNETT, E. BOUWS, H. CARLSON, D.E. CARTWRIGHT, H. ENKE, J.A. EWING, H. GIENAPP, D.E. HASSELMANN, P. KRUSEMAN, A. MEERBURG, P. MULLER, D.J. OLBERS, K. RICHTER, W. SELL and H. WALDEN (1973). Measurements of wind-wave growth and swell decay during the Joint North Sea Wave Project (JONSWAP). Deutsch. Hydrog. Z., A, 8(12).

HASSELMANN, K. (1974). On the spectral dissipation of ocean waves due to whitecapping. Boundary-Layer Met., 6, 107-127.

HASSELMANN, K., D.B. ROSS, P. MULLER and W. SELL. (1976). A parametrical wave prediction model. J. Phys. Oceanogr., 6, 201-228.

MILES, J.W. (1957). On the generation of surface waves by shear flow, 1. J. Fluid Mech., 3, 185-204.

RYE, H. (1977). The stability of some currently used wave parameters. Coastal Engineering, 1, 17-30.

* Internal reports of the Meteorological Office which may not be quoted without permission.

TABLE 1

Data losses during wave model calculations

(1) Data of 12 Z on 1 March 1980 and for 6 Z on 10 March 1980 are missing from the NORSWAM wave model data set.

(2) On four occasions the boundary data set or wind data set was lost. Remedial action taken was to use the most recent previous data as a substitute.

Boundaries missing:	00Z - 03Z on 15 March (3 hr. data sets)
	06Z - 09Z on 15 March.
Winds missing:	00Z - 06Z on 4 March (6 hr. data sets)
	18Z - 24Z on 24 March

(3) The wind data sets for 06Z-12Z, 12Z-18Z on 18 March were interchanged.

TABLE 2

Table of days in March 1980 when specified wind speed was exceeded

M/S	Brent B	Kinnairds Hd.	S. Uist	OWS Lima	DB1
25	0	0	0	2	0
20	3	0	0	4	2
15	9	2	2	11	9
10	22	9	13	26	23

TABLE 3

Wave model validation data

Station	Position	Wave Recorder	Length of record	Analysis method	Source of data
Brent B	61°04'N, 1°43'E	Waverider	20 min.	Wave processor	Shell U.K. Exploration & Production
Kinnaird's Head	57°59'N, 1°59'W	Waverider	17½ min.	Spectral analysis	I.O.S., Taunton
South Uist	57°18'N, 7°38'N	Waverider			
O.W.S. Lima	57°N, 20°W	SBWR			
DB1	48°42'N, 8°58'W	Datawell sensors	20 min.	Spectral analysis	UKOOA

TABLE 4

Parameters of least squares fit through the origin

Measurement station	Model	N_1	Correlation coefficient		Gradient of line (S.E.)		S.E. of residuals (% of mean)	
			h_s	P	h_s	P	h_s	P
Brent B	M	121	0.88	-	0.979(.02)	-	0.78(24)	-
	N	119	0.84	-	1.155(.03)	-	1.09(34)	-
Kinnaird's Head	M	76	0.86	0.87	0.914(.02)	0.851(.04)	0.51(22)	11.6(47)
	N	77	0.79	0.68	0.784(.03)	0.755(.06)	0.66(29)	19.6(80)
South Uist	M	85	0.75	0.66	1.195(.04)	1.272(.09)	1.09(43)	55.1(130)
	N	83	0.82	0.73	1.417(.04)	2.148(.15)	1.08(43)	84.4(202)
Lima	M	62	0.74	0.70	0.965(.03)	0.650(.06)	1.14(29)	62.7(71)
	N	61	0.82	0.76	1.084(.03)	1.186(.09)	1.10(28)	102.6(115)
DB 1	M	111	0.86	0.89	1.089(.03)	0.978(.04)	1.18(35)	78.3(90)
	N	109	0.84	0.82	1.268(.04)	1.373(.04)	1.53(45)	144.1(166)

Key: M = Met. Office

N = NORSWAM

TABLE 5

Parameters of general least squares fit

Measurement station	Model	Gradient of line (S.E.) h_s	Gradient of line (S.E.) P	Intercept (S.E.) h_s	Intercept (S.E.) P	S.E. of residuals (% of mean) h_s	S.E. of residuals (% of mean) P
Brent B	M	0.851(.04)	-	0.520(.07)	-	0.75(23)	-
	N	0.990(.06)	-	0.666(.10)	-	1.06(33)	-
Kinnaird's Head	M	0.883(.06)	0.743(.05)	0.084(.06)	5.27(1.3)	0.51(22)	11.1(45)
	N	0.880(.08)	0.745(.09)	-0.258(.07)	0.51(2.2)	0.66(29)	19.8(81)
South Uist	M	0.910(.09)	0.955(.12)	0.904(.11)	29.4(5.5)	1.02(40)	50.9(120)
	N	1.160(.09)	1.917(.20)	0.808(.11)	21.7(9.1)	1.02(41)	83.4(199)
Lima	M	0.530(.06)	0.402(.05)	2.03(.10)	55.5(5.8)	0.81(21)	45.5(51)
	N	0.843(.08)	1.065(.12)	1.12(.13)	27.6(12.9)	1.02(26)	101 (113)
DB 1	M	0.905(.05)	0.878(.04)	0.856(.10)	36.9(6.8)	1.09(32)	71.5(83)
	N	1.035(.07)	1.199(.08)	1.086(.14)	65.8(13)	1.42(42)	132 (152)

Ken: M = Met. Office

N = NORSWAM

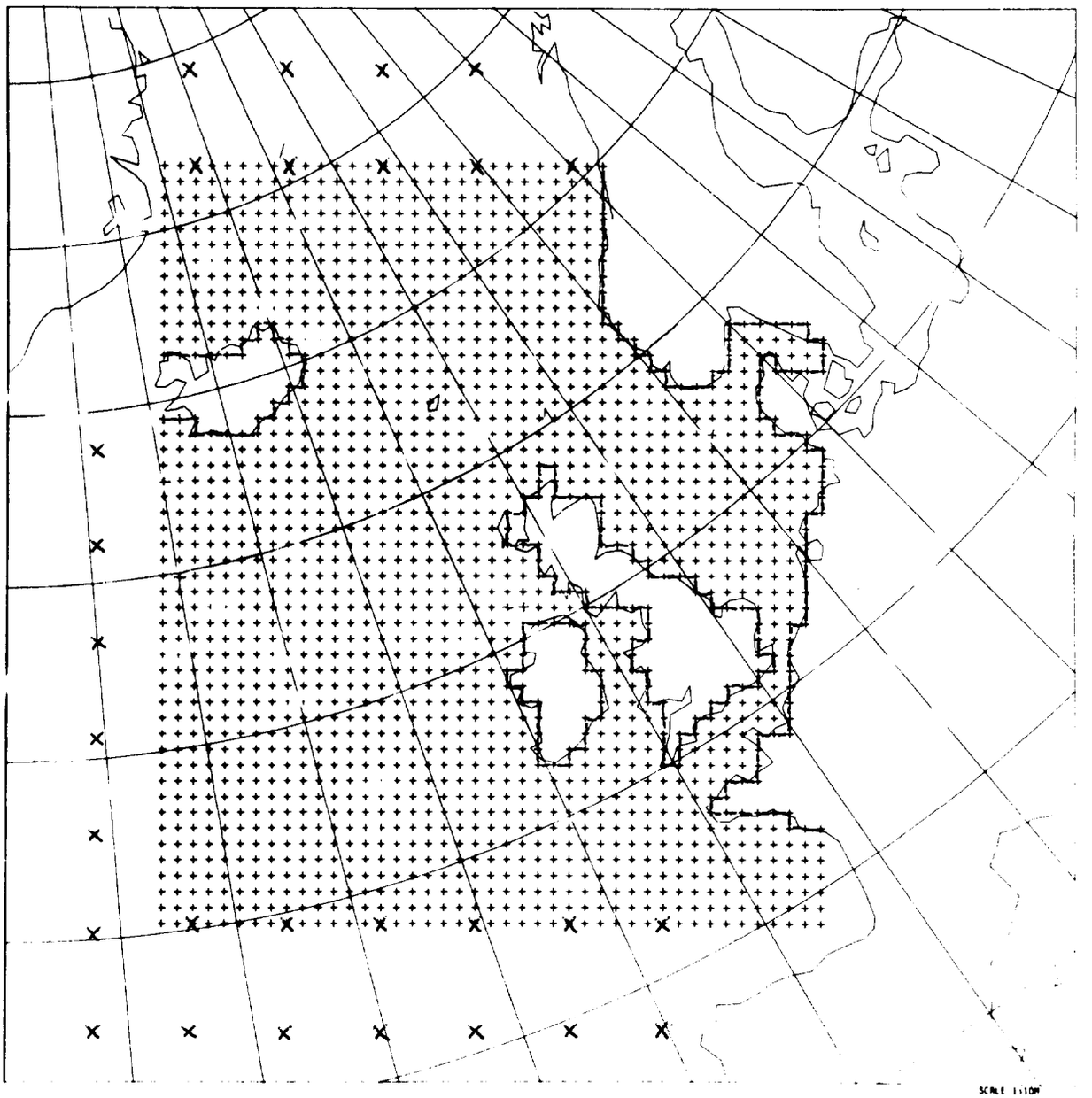

FIG. 1 Model grid scheme used for the computations

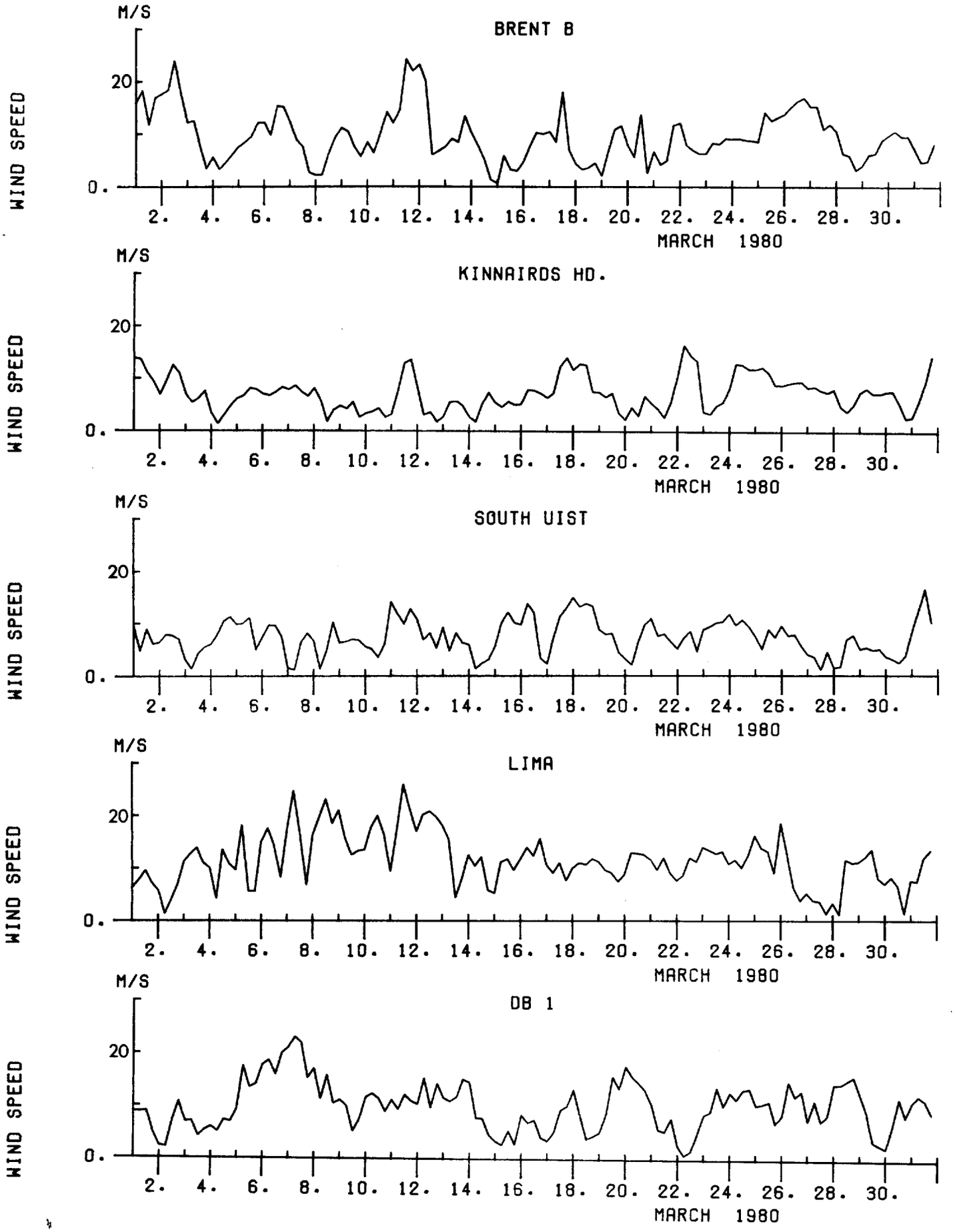

FIG. 2 Model wind speeds at the five wave measurement stations

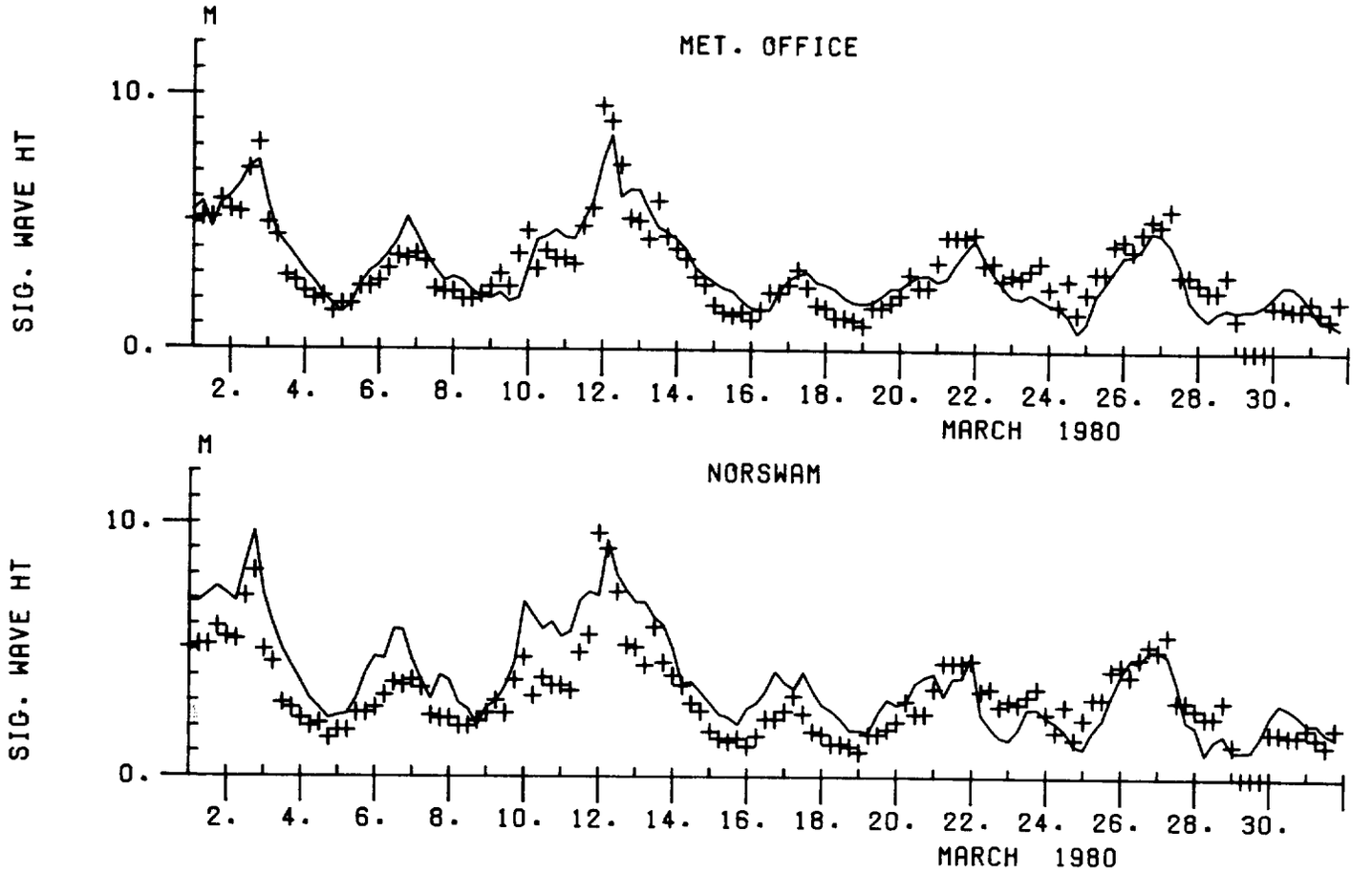

FIG. 3 Comparison of wave models (_____) with measured wave data (+) at Brent B.

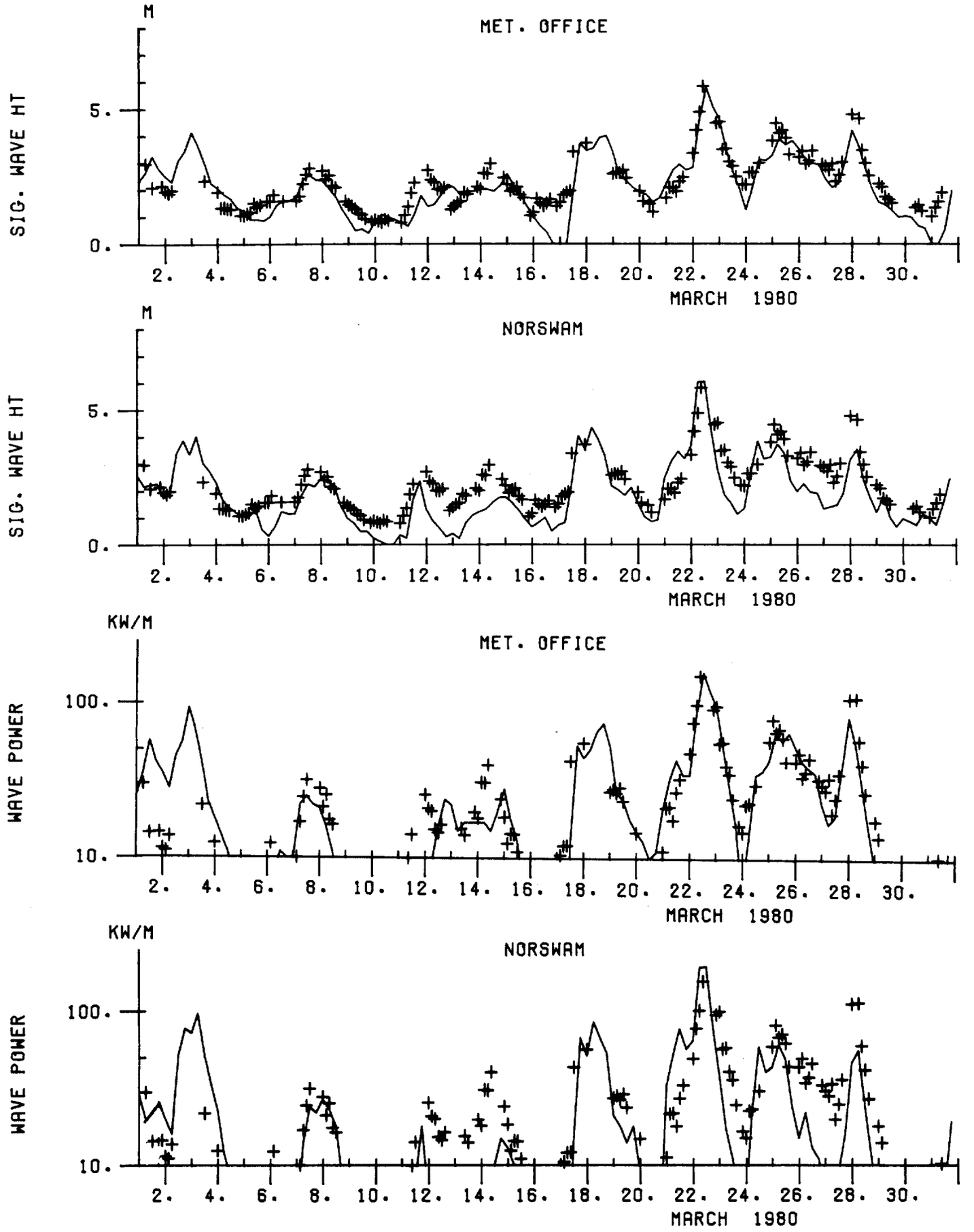

FIG. 4 Comparison of wave models (———) with measured wave data (+) at Kinnaird's Head.

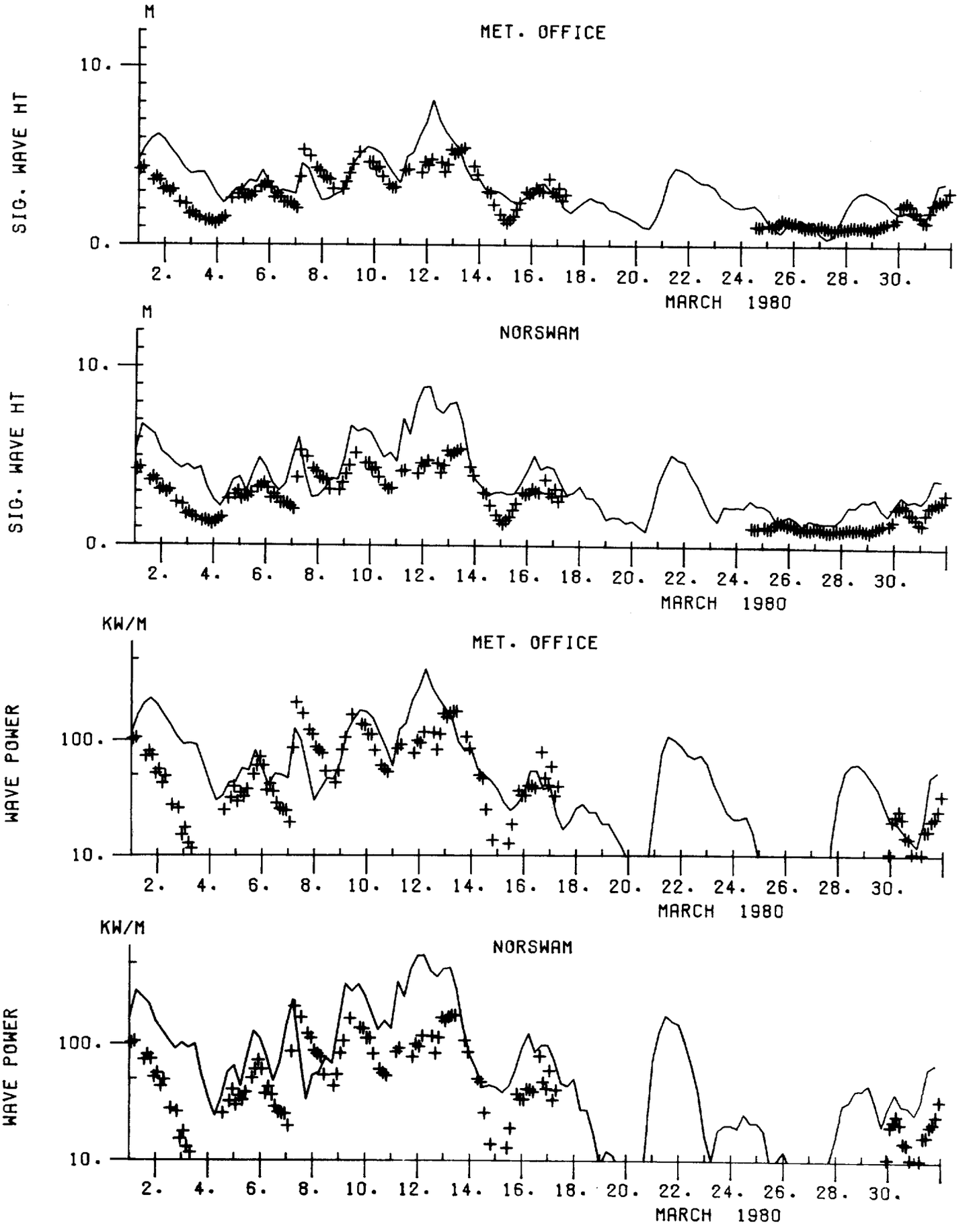

FIG. 5 Comparison of wave models (———) with measured wave data (+) at South Uist.

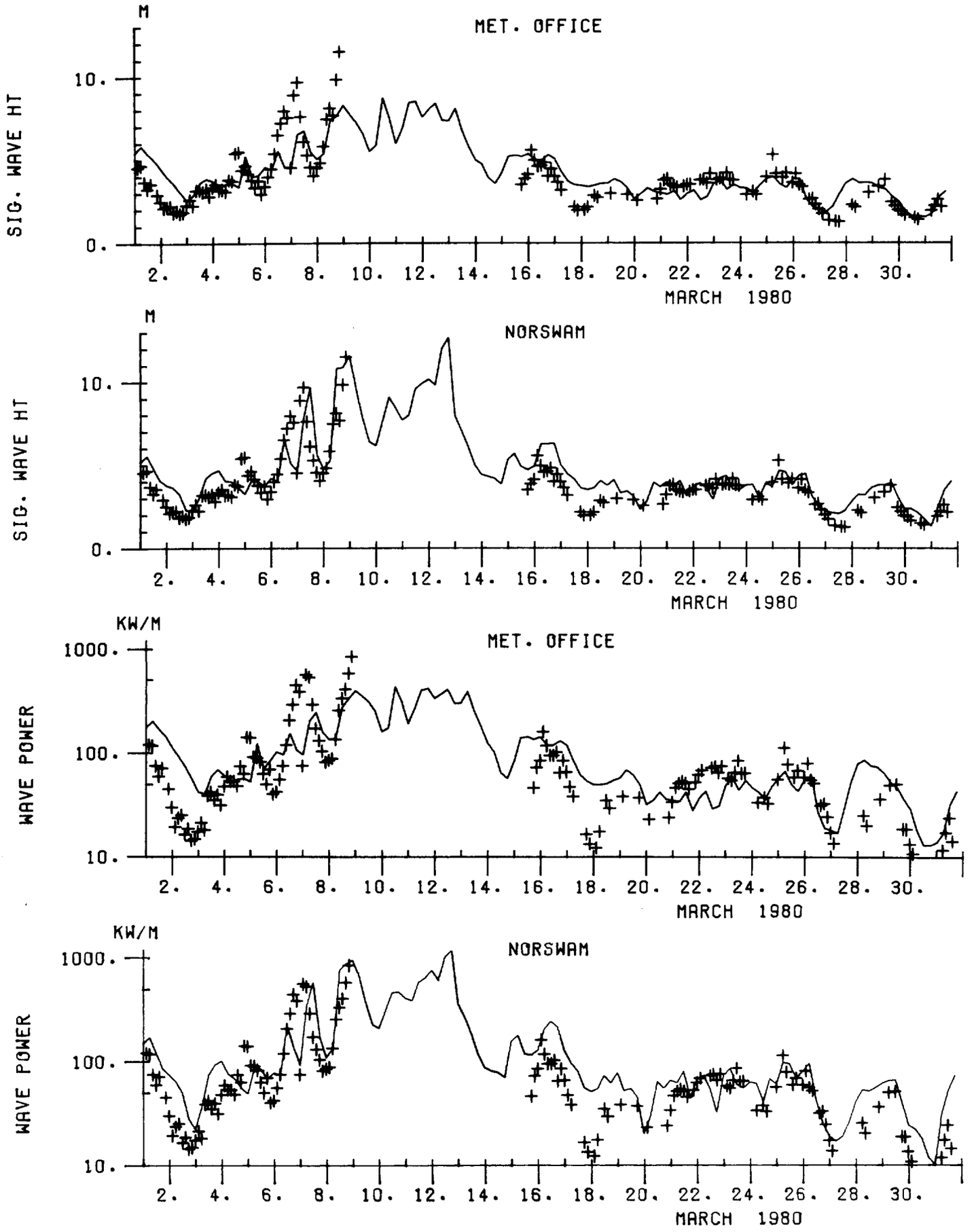

FIG. 6 Comparison of wave models (———) with measured wave data (+) at O.W.S. Lima

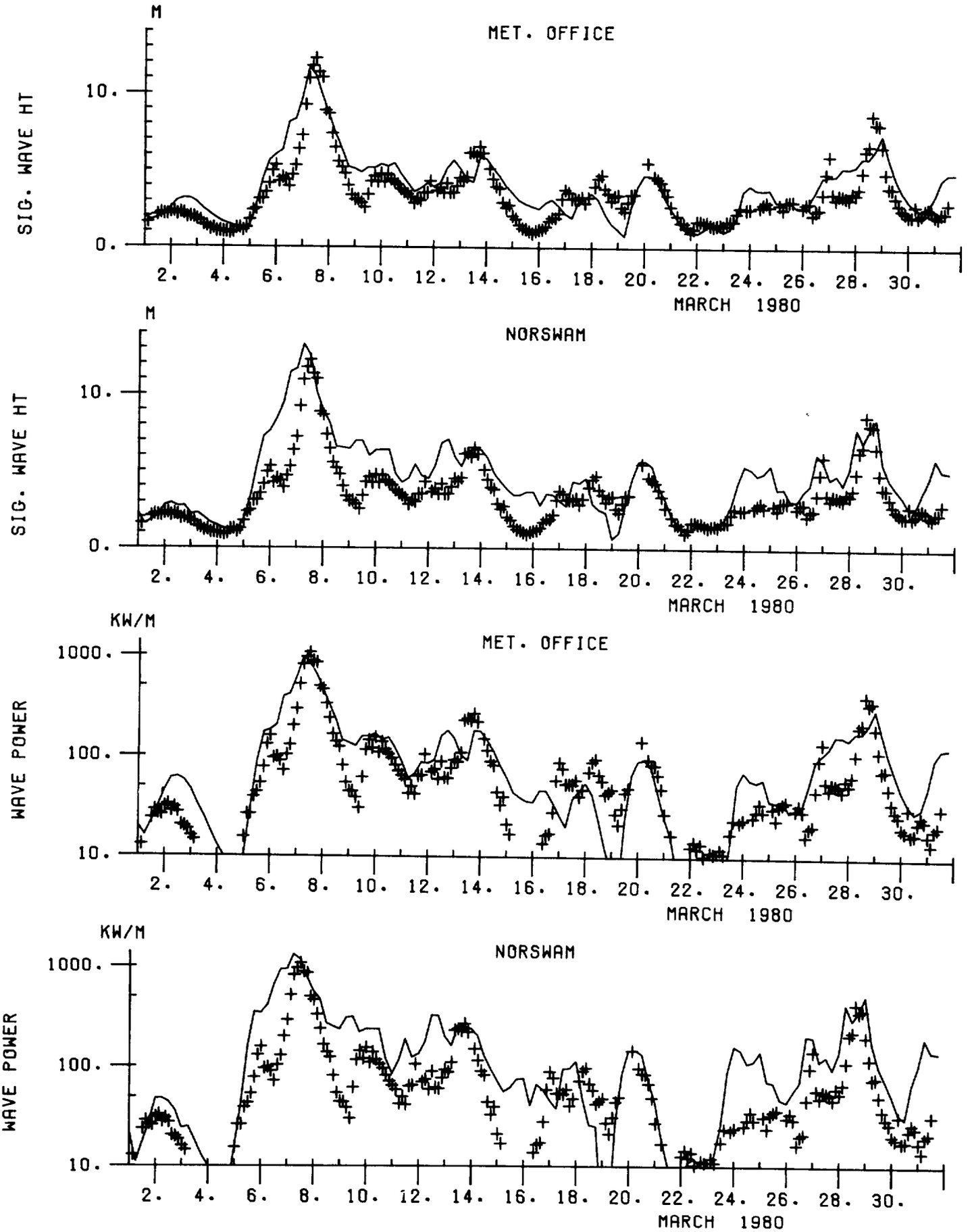

FIG. 7 Comparison of wave models (———) with measured wave data (+) at DB 1.

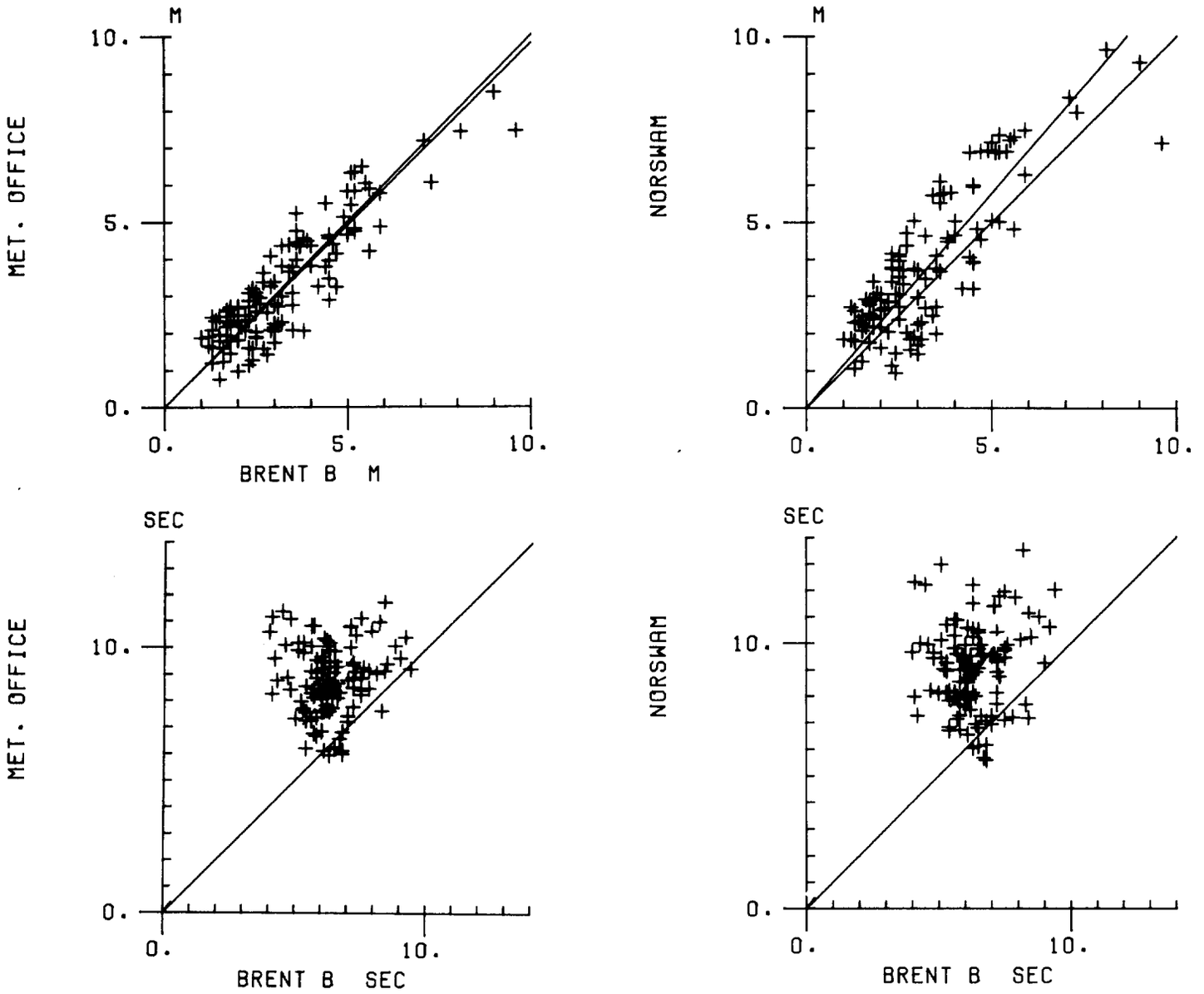

FIG. 8 Correlation of model and measured values at Brent B. The straight line corresponds to a 1:1 relation. For wave height only, the least squares fit through the origin is shown.

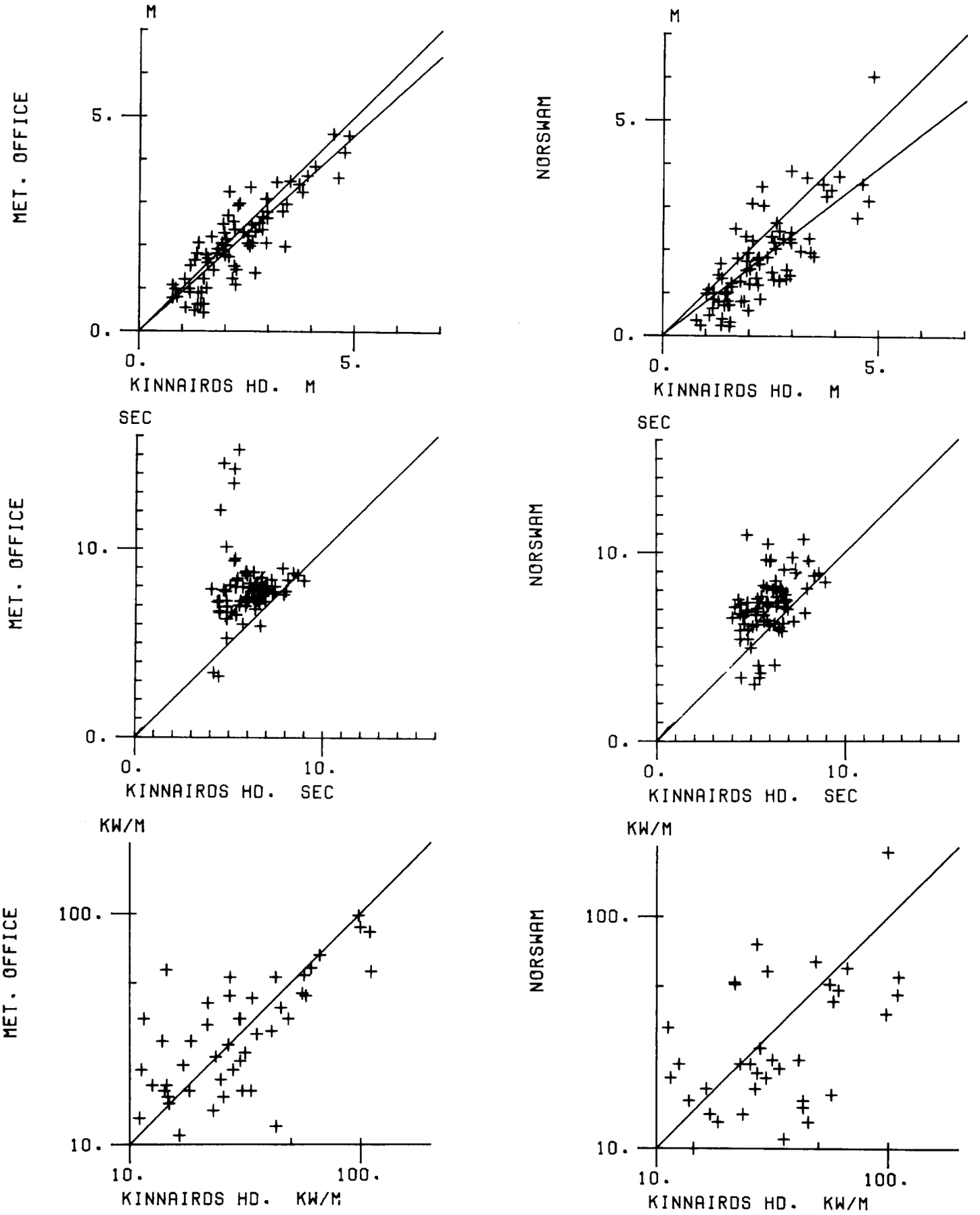

FIG. 9 Legend as for Fig. 8 but at Kinnaird's Head

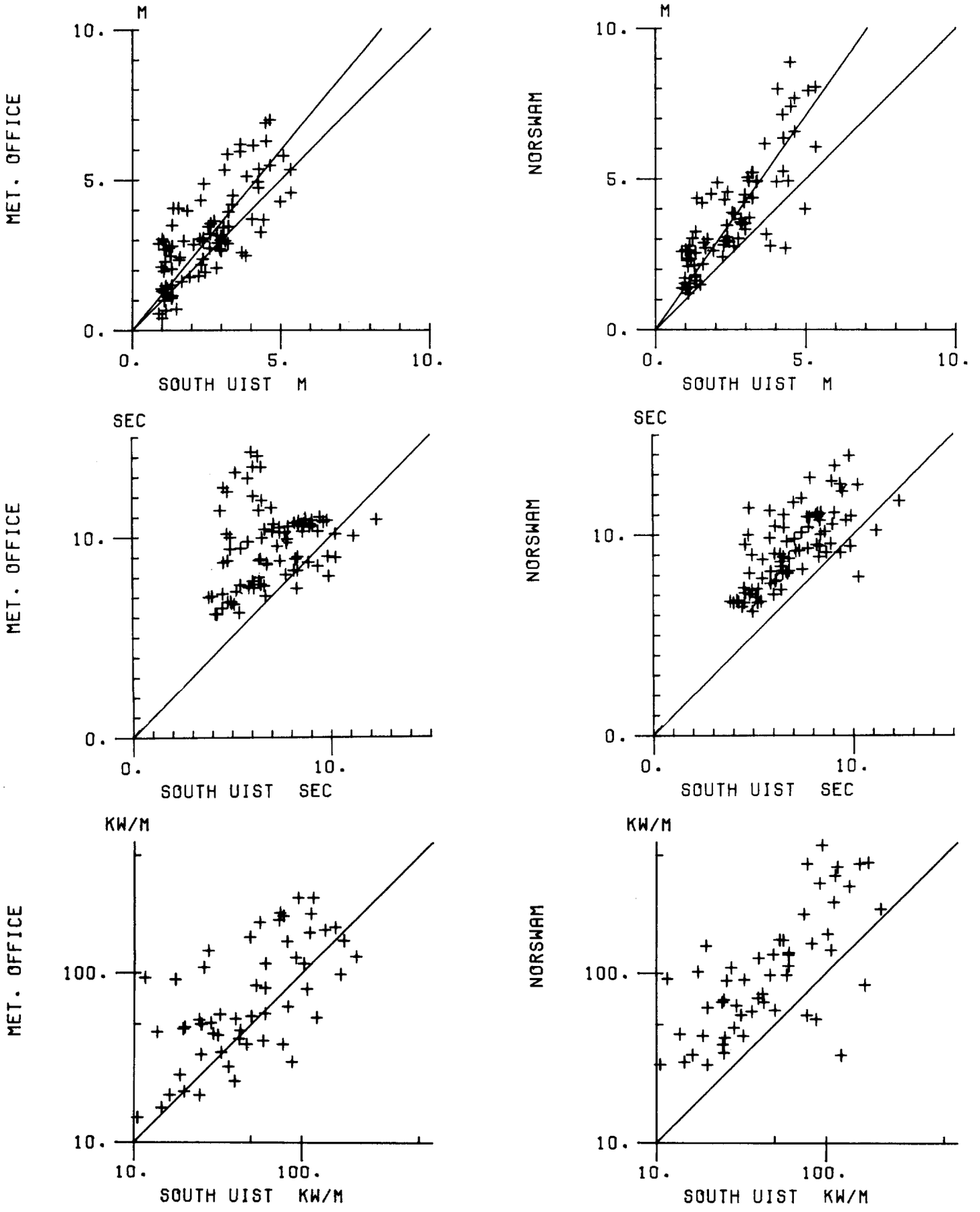

FIG. 10 Legend as for Fig. 8 but at South Uist

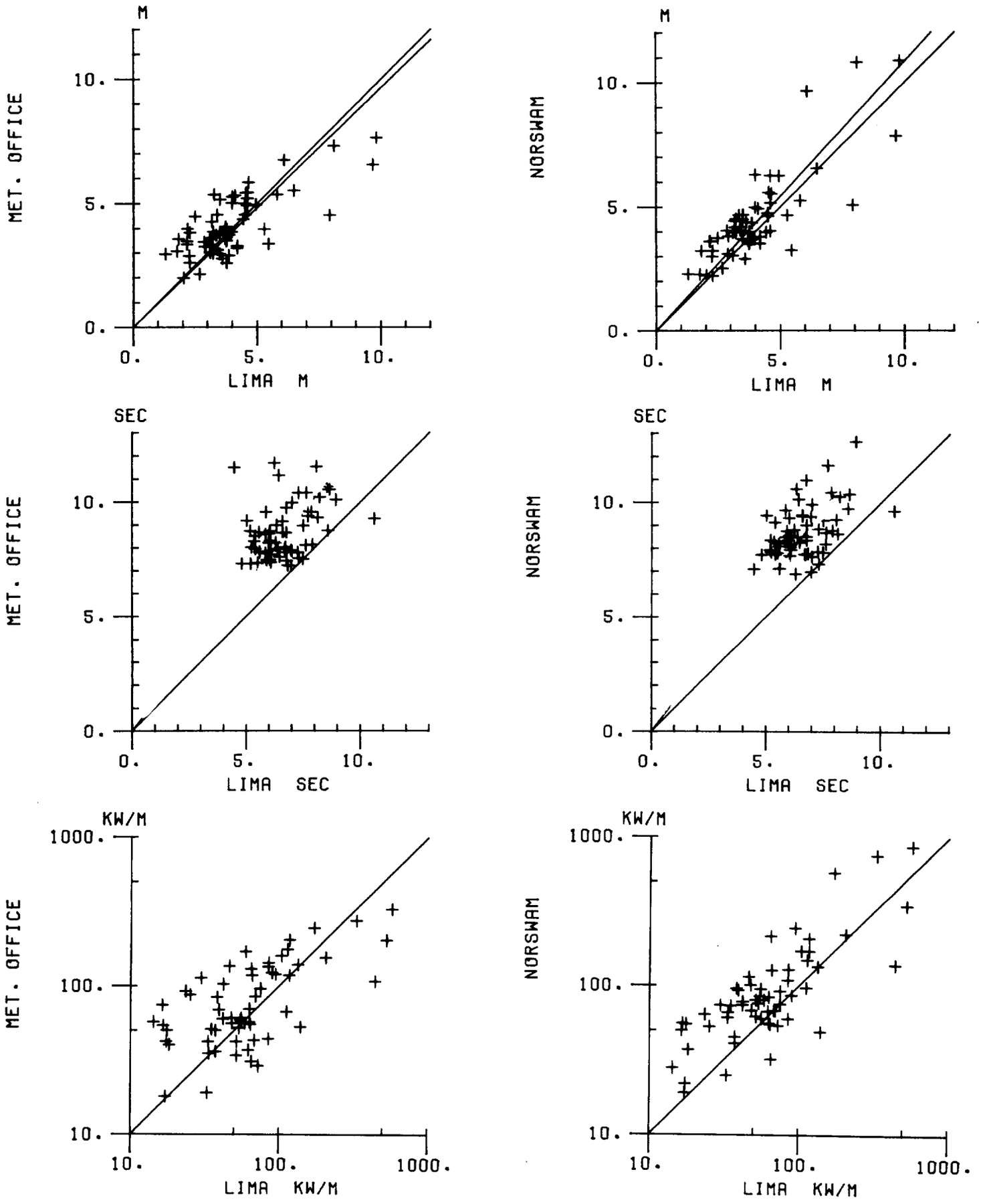

FIG. 11 Legend as for Fig. 8 but at O.W.S. Lima

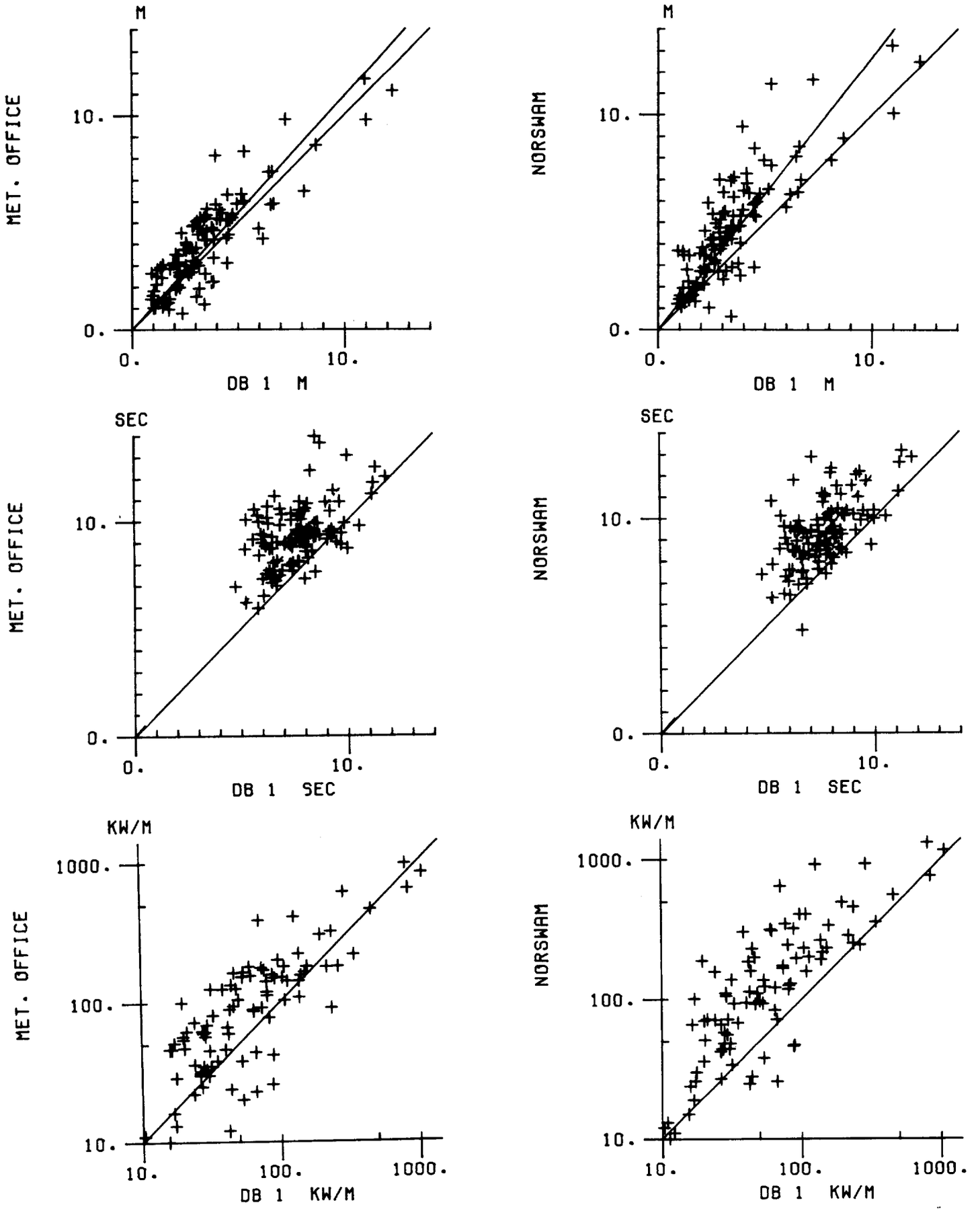

FIG. 12 Legend as for Fig. 8 but at DB 1.